Study of Interfacial Point Defects by Ballistic Electron Emission Microscopy

T. Meyer and H. von Känel

Laboratorium für Festkörperphysik, Eidgenössische Technische Hochschule Zürich-Hönggerberg, CH-8093 Zürich, Switzerland

(Received 2 December 1996)

Ballistic electron emission microscopy has been used to study individual point defects, which are located at the $CoSi_2/Si(111)$ interface of thin (~30 Å) silicide films grown epitaxially on silicon substrates by molecular beam epitaxy. Clear evidence for trapping of point defects at dislocations is presented. The lateral distribution of the interfacial point defects is explained in terms of diffusion during an annealing step in the growth process. [S0031-9007(97)02990-6]

PACS numbers: 61.72.Ji, 61.16.Ch, 68.35.Fx, 73.40.Ns

The invention of the scanning tunneling microscope (STM) has revolutionized the study of surface processes occurring during thin film growth. The anisotropy of surface diffusion in Si(100) homoepitaxial growth has been analyzed by STM [1] and the size and distribution of islands formed during growth at different temperatures has been used to extract data relevant for the nucleation process and the adatom diffusion at the surface [2]. Dendritic island growth caused by hindered adatom diffusion along step edges could be observed [3]. More recently adatom movements could be monitored in real time by this technique (see, e.g., [4]). While the STM's potential for real space surface studies thus appears evident, this is true to a far lesser extent for buried interfaces. An STM-based technique designed to close this gap has been invented by Kaiser and Bell [5]. It is called ballistic electron emission microscopy (BEEM) and allows the study of structures which influence the transmission of hot electrons across a metal-semiconductor interface (see, e.g., [6,7] for recent reviews). In BEEM the tip of a scanning tunneling microscope is used to inject hot electrons into a thin metallic film grown on top of a semiconducting collector. A fraction of these electrons is transmitted into the semiconductor and measured as the collector or BEEM current I_c. By registering I_c, while performing a normal STM scan, a BEEM image is obtained which renders information about the electron transmission across the metal/semiconductor interface. The transmission is affected by spatial variations of the barrier height, by elastic scattering at defects located at the surface, at the interface, or in the bulk of the film, or by a number of inelastic scattering processes [6,7]. Unlike Hallen *et al.* [8], who observed electron induced formation of atomic layers at a buried Au surface, we did not see any structural changes induced by electron irradiation. In an earlier Letter we have reported on the observation of hot electron scattering at individual misfit dislocations [9] located at the $CoSi_2/Si(111)$ interface. For the first time this allowed us to image interfacial dislocations by BEEM. In this Letter we show that under optimized conditions not only extended defects but even individual point defects can clearly be imaged by BEEM. Our new measurements show that the specific contrast formerly attributed to scattering at the dislocation cores must now be interpreted as scattering at individual point defects trapped within the cores. Furthermore, our experiments provide clear evidence for the lateral diffusion of point defects into the strain field region of misfit dislocations.

The samples were grown in a commercial VG MBE system at a base pressure of 10^{-10} mbar. First, a 3000-Å thick undoped silicon buffer layer was grown by molecular beam epitaxy (MBE) onto a $n^+(111)$-silicon substrate. Then the sample was flipped, and a thick $CoSi_2$ film was deposited in order to form an Ohmic back contact for the BEEM-current measurements. Subsequently, the sample was flipped a second time, and a thin silicide film (20–30 Å) forming the metallic base was grown. Both silicide films were grown using stoichiometric codeposition. After growth the samples were annealed at 640 °C for 5 min. Measurements were taken at 77 K in a home built low temperature STM suited for 3-in. wafers, which is located in the same UHV environment.

The lattice parameter a of cubic $CoSi_2$ is smaller than that of silicon by 1.2% at room temperature. From transmission electron microscopy (TEM) it is known that the strain in the silicide film is relaxed due to the presence of partial Shockley dislocations with a Burgers vector

$$\vec{b} = \frac{a}{6}\langle 11\bar{2}\rangle , \tag{1}$$

lying in the interfacial plane [10]. The dislocations are associated with an interfacial step. During the annealing process a quasihexagonal network of dislocations is formed. This network can be imaged by STM topography measurements because of a slight surface protrusion (0.6 Å) caused by the strain field of the dislocations. A topography and a BEEM image of such a network have been presented in Ref. [9].

In Fig. 1(a) a small-scale topography image featuring a single dislocation line is shown. In addition to the dislocation several surface point defects (labeled S) can be seen. As surface features may influence the energy and momentum distribution of the tunneling electrons (see [11]), they can be recognized in the BEEM image [Fig. 1(b)] as well. However, there are also bright,

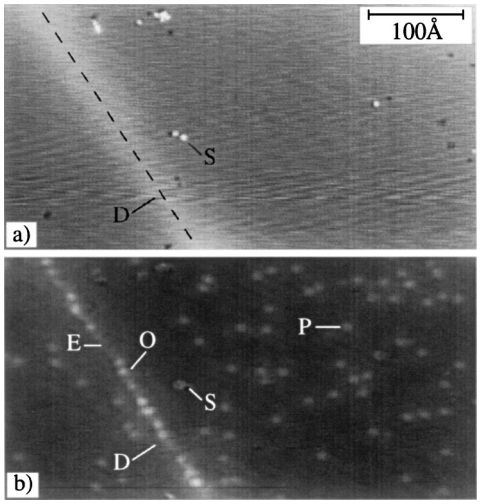

FIG. 1. (a) STM topography image of a 28-Å thick $CoSi_2$ film taken at ($V_t = -1.2$ V, $I_t = 20$ nA). The bright line (D) is a 0.6-Å high protrusion caused by the strain field of a dislocation. Some surface point defects are present (S). The gray scales range from 0 to 2 Å. (b) Corresponding BEEM image: interfacial point defects like the one labeled (P) have been trapped in the core of a dislocation (D). There are empty (E) and occupied (O) regions in the dislocation. The gray scales vary within a range of $\Delta I_c = 263$ pA.

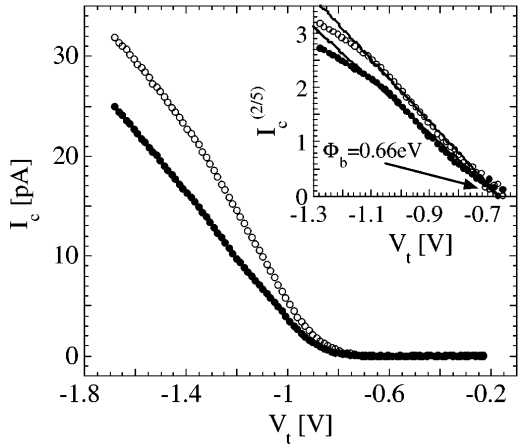

FIG. 2. Ballistic electron emission spectra normalized to a tunneling current $I_t = 1$ nA taken on top (∘) and next (•) to an interfacial point defect. I_c is higher on the defect for $V_t \rightarrow \Phi_b$. The inset shows the $\frac{2}{5}$-power of the collector current, yielding the same Schottky barrier of $\Phi_b = 0.66 \pm 0.01$ eV.

pointlike contrast features in the BEEM image which cannot be associated with a surface defect: these spots of enhanced collector current are about 10 Å in diameter and appear to be nearly uniformly distributed.

At a defect-free epitaxial interface only electrons which fulfill the kinematic matching conditions (e.g., energy above the Schottky barrier and conservation of the in-plane component of the wave vector) are expected to be transmitted into the semiconducting collector. Scanning with a constant tunneling current yields images of I_c, an example of which is shown in Fig. 1(b). Measurements of the collector current as a function of tunneling bias (ballistic electron emission spectroscopy or BEES in short) are used to determine the height of the Schottky barrier. This has been done for the $CoSi_2$/Si(111) interface with the result that the barrier is homogeneous all over the interface (including the regions of dislocations and point defects). As an example ballistic electron emission spectra taken on top of a point defect and in the defect-free region in its vicinity are compared in Fig. 2. Whereas the Schottky barrier is found to be the same ($\phi_B = 0.66$ eV) within the experimental error of ± 0.01 eV, I_c is enhanced over the point defect right down to the onset. In view of the constant barrier, the local increase of the collector current must be due to an enhancement of the electron transmission probability at the interface induced by scattering of electrons at an interfacial object. This may be understood in the following way (for a more detailed description, see, e.g., [12]): Electrons injected by an STM tip are strongly focused forward, which means that their distribution of in-plane momentum $k_\parallel$ is peaked at $k_\parallel = 0$. On the other hand, the barrier at the metal/semiconductor interface is lowest for electrons which have $k_\parallel \approx 0.8$ Å^{-1}, matching the position of the silicon conduction band minima (CBM). Hence only if an electron experiences an elastic scattering event at the interface can it pick up the lateral momentum required to reach the silicon CBM. Scattering centers at the interface will therefore increase the electron transmission and show up as bright contrast in a collector-current image. Although in principle scattering could take place anywhere in the film there are several arguments favoring the interpretation that the bright spots in a BEEM image are due to scattering centers located at the interface.

(i) Surface scattering can be excluded since surface defects (like the one indicated in Fig. 3 by S) should show up in atomically resolved topography images.

(ii) The nearly uniform and exceedingly small size of the defects (≈10 Å) renders it highly unlikely that the latter are located between the metallurgical interface and the potential maximum within the silicon.

(iii) The small correlation length for surface roughness deduced from resistivity measurements requires the presence of additional scattering centers apart from steps [13].

(iv) Finally, band structure calculations by Stiles and Hamann [14]—if applicable—indicate also that the point defects are located right at the interface. According to these calculations there are no states in $CoSi_2$, which match the silicon conduction band minima in the vicinity of the Schottky barrier. For this reason the onset of the BEEM current should be delayed if conservation of parallel momentum at the interface was strictly valid. The fact that we do not observe the delayed onset—even in spectra taken in defect-free regions—suggests a small, but finite scattering probability everywhere at the epitaxial interface [15]. One possible mechanism might be electron-phonon

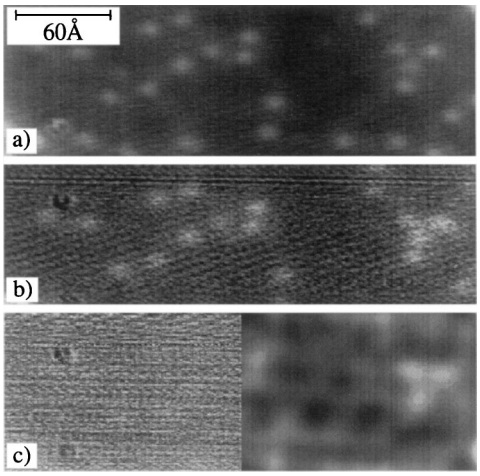

FIG. 3. (a) BEEM image taken at a tip voltage of $V_t = -1.2$ V. (b) BEEM image taken shortly afterwards with $V_t = -0.8$ V. The contrast due to scattering at point defects is still visible at low tip bias, indicating that these are located at the interface and not within the $CoSi_2$ layer. (c) At $V_t = -0.7$ V the contrast caused by the point defects has disappeared in the noise (left), but can still be found by low-pass filtering the image (right). The tunneling current was $I_t = 20$ nA and the gray scales vary within a range of $\Delta I_c = 200$ pA (a), $\Delta I_c = 40$ pA (b), $\Delta I_c = 16$ pA [(c), left], and $\Delta I_c = 3$ pA [(c), right].

scattering [16]. Since scattering within the $CoSi_2$ cannot increase the transmission probability close to ϕ_B, the BEEM contrast due to objects located in the bulk of the film should vanish as the tip bias is lowered towards ϕ_B. BEES taken on a subsurface point defect and in its neighborhood (Fig. 2) does not, however, reveal any diminishing contrast as the electron energy approaches ϕ_B. This can also be seen in Fig. 3, where BEEM images taken at the same location with different tip biases are shown. The point defects are clearly visible for $V_t = -1.2$ V in Fig. 3(a). For $V_t = -0.8$ V in Fig. 3(b) the contrast due to scattering at point defects is still above the noise level. For still lower electron energy ($V_t = -0.7$ V) the scattering contrast disappears in the noise [see Fig. 3(c) left]. It can be made visible by low-pass filtering the image [see right hand side of Fig. 3(c)].

On closer inspection of the dislocation in Fig. 1(b), it is evident that the contrast is not uniform along this line. On the contrary, the BEEM current is largest at point defects which have accumulated in the core of the dislocation. This becomes even more evident from a comparison of line sections taken across the dislocation line (Fig. 4), either through an empty region of the core (E) or at a site occupied by a point defect (O). Hardly any scattering contrast is found at location (E), whereas I_c is strongly enhanced close to (O). In view of these new results the sharp linear contrast features previously observed in BEEM images [9] can no longer be attributed to scattering at the dislocation core. The contrast must have been due to scattering at unresolved point defects accumulated in

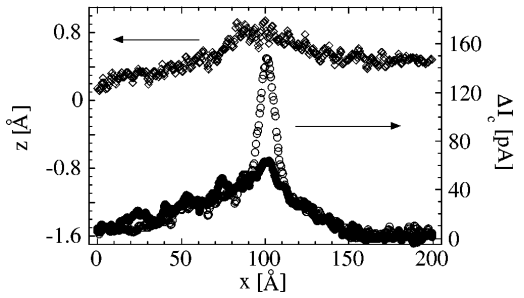

FIG. 4. Line sections taken orthogonal to the dislocation line shown in Fig. 1 through the points indicated E and O. The BEEM current is enhanced at the location O, where a point defect is present (see ∘). The current in the line section which does not pass through a point defect (•) shows only a faint variation on a length scale comparable to the surface deformation (◇).

the dislocation core. The long range variation of the collector current visible across the "empty" site (E) and the deformation of the surface occur on exactly the same length scale (FWHM = 60 Å), which is given by the extent of the dislocation's strain field. This long range contrast is not due to scattering at a point defect or the dislocation core but related to the strain field.

In all the BEEM images the density of point defects is found to be lower close to the dislocation lines. Evaluating several images from scans made at a larger scale than that of Fig. 1(b), the point defect density, n, as a function of distance from the closest dislocation line was obtained (see Fig. 5). These data were fitted with a simple one-dimensional model, in which diffusion of point defects into a perfect sink at $x = 0$, the core of the dislocation, was assumed. A uniform concentration n_0 of point defects in the interfacial plane was taken as a starting condition, leading to the following expression for n:

$$n = n_0 \operatorname{erf}\left(\frac{x}{2\sqrt{Dt}}\right). \tag{2}$$

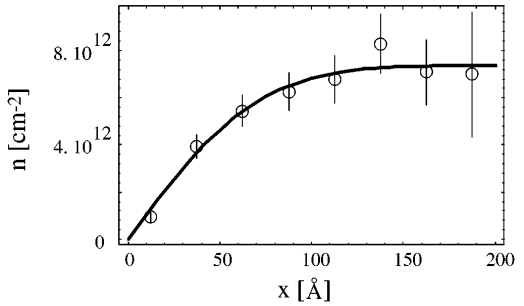

FIG. 5. Point defect density n plotted as a function of distance x from a dislocation. The solid line is a solution to the one-dimensional diffusion equation obtained by assuming a constant initial concentration of point defects and a perfect sink at $x = 0$. The fit yields an initial density $n_0 = 7.37 \times 10^{12}$ cm^{-2} and a diffusion coefficient of 5.2×10^{-16} cm^2 s^{-1}.

It was further assumed that diffusion takes place during the final annealing step (after growth), during which the sample is kept at a temperature of 640 °C for a time t of about 5 min. A diffusion coefficient D of 5.2×10^{-16} cm^2 s^{-1} and an initial point defect density of $n_0 = 7.37 \times 10^{12}$ cm^{-2} was obtained. Summing up the missing point defects next to a dislocation line, we expect to find them trapped in the core of the dislocation at a line density of 0.066 Å^{-1}. Counting all point defects in several highly resolved BEEM images of dislocations yielded an occupation of 0.0626 ± 0.01 Å^{-1} in very good agreement with the value derived from the fit.

The BEEM contrast stemming from a single point defect has a width of approximately 10 Å. This width is a convolution of the actual size of the scatterer and the width of the electron beam at the interface. Since it reflects changes in tunneling and tip conditions it is merely an indicator of the width of the electron beam. The scattering object at the interface itself is considered to be of atomic size. Unfortunately, the present measurements do not render any further information about the structural nature of the point defects observed by BEEM. It is therefore a matter of speculation, whether the scattering is caused by vacancies, interstitial defects, or impurity atoms. One argument in favor of identifying the point defects with vacancies is the following: When the silicide crystallizes from the as-deposited amorphous phase in the first stage of the annealing it assumes a defect CsCl-type crystal structure, in which only half of the Co sublattice is occupied by randomly distributed Co atoms [17,18]. Upon further annealing this phase is transformed to the bulk-stable $CoSi_2$ phase with the CaF_2 crystal structure. It appears likely that this process will leave some Co vacancies at the interface. Such a distribution of (presumably magnetic) defects in the Co sublattice at the interface could also account for the enhanced magnetic scattering observed in transport measurements performed on thin $CoSi_2$ films [19,20]. A vacancy can be considered a region of lowered strain and is attracted to regions of compressive strain (see, e.g., [21]). An accumulation of vacancies near the core of a dislocation line is energetically favorable.

When measuring point defect densities in the range of 10^{12}–10^{13} cm^{-2}, the BEEM technique has a big advantage over techniques like cross-sectional STM or TEM. By using one of these techniques it is very hard to obtain statistically relevant data on the lateral variation of point defect density, because the mean distance between two point defects appearing in the image of a cross section is of the order of 100 Å. This is comparable to the spacing between dislocation lines of typically 400–500 Å, which would render it difficult to measure the point defect density as a function of distance from dislocation cores.

The authors thank H.-U. Nissen for valuable discussions and critical reading of the manuscript. Financial support from the Swiss National Science Foundation is gratefully acknowledged.

[1] Y.-W. Mo, R. Kariotis, D. E. Savage, and M. G. Lagally, Surf. Sci. **219**, L551 (1989).
[2] J. A. Stroscio and D. T. Pierce, Phys. Rev. B **49**, 8522 (1994).
[3] T. Michely, M. Hohage, M. Bott, and G. Comsa, Phys. Rev. Lett. **70**, 3943 (1993).
[4] B. S. Swartzentruber, Phys. Rev. Lett. **76**, 459 (1996).
[5] W. J. Kaiser and L. D. Bell, Phys. Rev. Lett. **60**, 1406 (1988).
[6] L. D. Bell and W. J. Kaiser, Annu. Rev. Mater. Sci. **26**, 189 (1996).
[7] M. Prietsch, Phys. Rep. **253**, 163 (1995).
[8] H. D. Hallen, T. Huang, A. Fernandez, J. Silcox, and R. A. Buhrman, Phys. Rev. Lett. **69**, 2931 (1992).
[9] H. Sirringhaus, E. Y. Lee, and H. von Känel, Phys. Rev. Lett. **73**, 577 (1994).
[10] C. W. T. Bulle Lieuwma, D. E. W. Vandenhoudt, J. Henz, N. Onda, and H. von Känel, J. Appl. Phys. **73**, 3220 (1993).
[11] H. Sirringhaus, E. Y. Lee, and H. von Känel, Phys. Rev. Lett. **74**, 3999 (1995).
[12] A. Fernandez, H. D. Hallen, T. Huang, R. A. Buhrman, and J. Silcox, Phys. Rev. B **44**, 3428 (1991).
[13] H. von Känel and G. Fishman, Phys. Rev. B **45**, 3929 (1992).
[14] M. D. Stiles and D. R. Hamann, J. Vac. Sci. Technol. B **9**, 2394 (1991).
[15] The delayed onset observed in earlier *ex situ* experiments [see W. J. Kaiser, M. H. Hecht, R. W. Fathauer, L. D. Bell, E. Y. Lee, and L. C. Davies, Phys. Rev. B **44**, 6546 (1991)] could not be confirmed by our locally resolved spectroscopy performed in UHV nor by Palm *et al.* [see H. Palm, Ph.D. thesis, Universität Erlangen, 1994)]. We have indications for a small scattering probability everywhere at the interface (see [16]).
[16] H. Sirringhaus, T. Meyer, E. Y. Lee, and H. von Känel, Phys. Rev. B **53**, 15 944 (1996).
[17] C. Pirri, S. Hong, M. H. Tuilier, P. Wetzel, and G. Gewinner, Phys. Rev. B **53**, 1368 (1996).
[18] H. von Känel, E. Müller, S. Goncalves-Conto, C. Schwarz, and N. Onda, Surf. Sci. (to be published).
[19] J. F. DiTusa and J. M. Parpia, Appl. Phys. Lett. **57**, 452 (1990).
[20] J. Y. Veuillen and J. Derrien, Appl. Phys. Lett. **51**, 1448 (1987).
[21] A. H. Cottrell, *Dislocations and Plastic Flow in Crystals* (Clarendon Press, Oxford, 1953).